New Phytologist

Research

THERMOSENSITIVE BARREN PANICLE (TAP) is required for rice panicle and spikelet development at high ambient temperature

Peng Zhang[1], Wanwan Zhu[1], Yi He[1], Junyi Fan[1], Jin Shi[1], Ruifeng Fu[1], Jianping Hu[2], Li Li[3], Dabing Zhang[1] and Wanqi Liang[1]

[1]Joint International Research Laboratory of Metabolic & Developmental Sciences, State Key Laboratory of Hybrid Rice, School of Life Sciences and Biotechnology, Shanghai Jiao Tong University, Shanghai 20040, China; [2]Department of Energy Plant Research Laboratory and Plant Biology Department, Michigan State University, East Lansing, MI 48824, USA; [3]State Key Laboratory of Hybrid Rice, Hunan Hybrid Rice Research Center, Hunan Academy of Agricultural Sciences, Changsha 410125, China

Author for correspondence:
Wanqi Liang
Email: wqliang@sjtu.edu.cn

Received: *24 July 2022*
Accepted: *5 October 2022*

New Phytologist (2022)
doi: 10.1111/nph.18551

Key words: FAR1-RELATED SEQUENCE protein, high ambient temperature, OsYABBY, panicle, rice (*Oryza sativa*), spikelet.

Summary

- In cereal plants, the size of the panicle (inflorescence) is a critical factor for yield. Panicle size is determined by a complex interplay of genetic and environmental factors, but the mechanisms underlying adaptations to temperature stress during panicle development remain largely unknown.
- We identify the rice *THERMOSENSITIVE BARREN PANICLE* (*TAP*) gene, which encodes a transposase-derived FAR1-RELATED SEQUENCE (FRS) protein and is responsible for regulating panicle and spikelet development at high ambient temperature. The *tap* mutants display high temperature-dependent reproductive abnormalities, including compromised secondary branch and spikelet initiation and pleiotropic floral organ defects. Consistent with its thermosensitive phenotype, *TAP* expression is induced by high temperature.
- TAP directly promotes the expression of *OsYABBY3* (*OsYAB3*), *OsYAB4*, and *OsYAB5*, which encode key transcriptional regulators in panicle and spikelet development. In addition, TAP physically interacts with OsYAB4 and OsYAB5 proteins; phenotypic analysis of *osyab4 tap-1* and *osyab5 tap-1* double mutants indicates that TAP–OsYAB4/OsYAB5 complexes act to maintain normal panicle and spikelet development.
- Taken together, our study reveals the novel role of a TE-derived transcription factor in controlling rice panicle development under high ambient temperatures, shedding light on the molecular mechanism underlying the adaptation of cereal crops to increasing environmental temperatures.

Introduction

Temperature is one of the most important environmental factors that affect plant growth. Global warming has increased the frequency of heat stress events, with deleterious effects on crop yields. Although the complex and sophisticated mechanisms that allow plants to adapt to high temperature have been extensively studied during vegetative growth (Wigge, 2013), much less is known about these mechanisms during plant reproductive growth, especially during early reproductive development that is highly vulnerable to temperature stresses.

Cereal crop yields largely depend on the size of plant panicles (inflorescences) and the number of attached spikelets that produce grain-bearing florets. The reduction in crop yield under adverse conditions is mostly due to a decrease in grain number rather than grain weight (Cao *et al.*, 2009). In rice, high temperatures during panicle initiation can cause a significant loss of grain number due to interrupted differentiation of secondary branches and spikelets (Wu *et al.*, 2016, 2019). In wheat and barley, high ambient temperatures lead to delayed panicle (inflorescence) meristem development and reduced numbers of spikelet primordia (Jacott & Boden, 2020). Recent studies have started to unravel the mechanisms and key thermosensitive regulators in early inflorescence development. Our work in barley demonstrated the role of the SEPALLATA MADS-box protein HvMADS1 in maintaining unbranched inflorescence architecture at high temperatures (Li *et al.*, 2021); higher temperatures induce conformational changes in target promoters that promote HvMADS1 binding and activation. The maize *thermosensitive vanishing tassel1-R* (*tvt1-R*) mutant lacks tassels at high temperatures due to arrested development of the shoot apical meristem; the causative mutation in *ZmRNRL1* compromises the rate of deoxyribonucleoside triphosphate (dNTP) production, and therefore DNA synthesis, in a temperature-dependent manner (Xie *et al.*, 2020). No such thermosensitive regulators of spikelet or inflorescence development have previously been reported in rice.

Rice plants develop a determinate compound panicle structure, in which the central rachis bears several primary branches generated from the panicle meristem. After generating one or several secondary branch meristems, the primary branch meristem is converted to a terminal spikelet meristem. Meristems that generate spikelets are directly initiated on the primary and secondary branches (Zhang & Yuan, 2014; Yuan *et al.*, 2020). The spikelet

meristem produces a defined number of floral organs, including the lemma, palea, lodicule, stamen, and pistil (Ikeda *et al.*, 2004; Itoh *et al.*, 2005). Rice panicle architecture and grain number therefore rely on correct and coordinated meristem activity, which is controlled by a complex network of transcriptional regulation and hormone signaling pathways (Yuan *et al.*, 2020).

The YABBY (YAB) proteins comprise a flowering plant-specific family of transcription factors that regulate plant development, morphogenesis, and stress responses (Zhang *et al.*, 2020; Palermo & Dornelas, 2021); members of the rice OsYAB family have been reported to play a role in panicle and spikelet development (Yamaguchi *et al.*, 2004; Tanaka *et al.*, 2012, 2017). YAB proteins are characterized by two conserved domains: an N-terminal C_2H_2 zinc-finger domain and a C-terminal helix–loop–helix domain, that is, the YABBY domain (Bowman & Smyth, 1999). YAB proteins in dicotyledonous angiosperms are divided into five subfamilies: CRABS CLAW (CRC), FILAMENTOUS FLOWER (FIL)/YAB3, INNER NO OUTER (INO), YAB2, and YAB5. Monocotyledonous rice lacks the YAB5 subfamily (Toriba *et al.*, 2007).

The FIL/YAB3 subfamily is involved in floral organ development and establishment of inflorescence architecture. The *fil* mutants in *Arabidopsis* exhibit filamentous floral organs, flowers with altered shape and number of floral organs, and immature flowers arrested in development (Chen *et al.*, 1999). The rice genome contains three *FIL/YAB3* genes: *TONGARI-BOUSHI1* (*TOB1* or *OsYAB5*), *OsYAB4* (*TOB2*), and *OsYAB3* (*TOB3*) (Toriba *et al.*, 2007), all of which are uniformly expressed in the lateral organ primordia. Although the rice *FIL/YAB3* subfamily members do not exhibit polar expression of their *Arabidopsis* orthologs, they share similar functions in regulating floral organ development and inflorescence architecture. Disruption of *TOB1* led to developmental defects in spikelets and partial loss of floral meristem identity (Tanaka *et al.*, 2012), and simultaneous RNAi knockdown of *TOB2* and *TOB3* in *tob1* led to small panicles that bear naked branches without spikelets (Tanaka *et al.*, 2017), suggesting partial functional redundancy of the three *TOBs* in initiating and maintaining the branch and spikelet meristems. The mechanism(s) underlying the regulatory role of *FIL/YAB* genes in rice panicle and spikelet development remain to be elucidated.

Increasing evidence shows that transposable element (TE)–derived genes can be sources for beneficial agronomic traits and adaptive functions in crops in response to changing environments (Lin *et al.*, 2007; Fedoroff, 2012). One such protein family is the FAR-RED IMPAIRED RESPONSE1 (FAR1)-related sequences (FRS) family of transcription factors in *Arabidopsis* (Hudson *et al.*, 2003). *Arabidopsis* FAR1 and FAR-RED ELONGATED HYPOCOTYLS3 (FHY3) are homologous FRS proteins that participate in a wide range of cellular processes, including signal transduction in photomorphogenesis (Hudson *et al.*, 1999, 2003), circadian clock regulation (Allen *et al.*, 2006; Li *et al.*, 2011), chloroplast division (Chang *et al.*, 2015), abscisic acid signaling (Tang *et al.*, 2013), and shoot meristem and floral development (Stirnberg *et al.*, 2012; Li *et al.*, 2016; Liu *et al.*, 2016). Despite the higher number of *FRS* genes in monocot genomes, their functions are poorly understood. In *Poaceae* grasses, *Mutator-like* transposable element (MULE)-derived transcription factors form clades that contain monocot-specific FAR1 domains, suggesting that these genes may have evolved to play monocot-specific roles in response to environmental cues (Song & Cao, 2017).

Here, we reveal that TAP, a member of the rice FRS protein family, is required for normal reproductive growth in response to high ambient growth temperatures. At high ambient temperature, TAP acts by itself and together with OsYAB proteins to control panicle and spikelet development through the regulation of gene expression. Our study provides further evidence that transposase-derived genes have been powerful contributors to plant adaption to climate change in the past and may be critical tools to accelerate breeding outcomes for the future.

Materials and Methods

Plant materials and generation of transgenic plants

Rice (*Oryza sativa* ssp. *japonica*) cultivar 9522 plants were used in this study. The *tap-1* mutant was isolated from a mutant population generated by treating the seeds of 9522 with 60Co γ-irradiation (Wang *et al.*, 2006). Other mutant lines (*tap-2, tap-3, osyab4, osyab5, and osyab4 osyab5*) were generated using CRISPR/Cas9 in 9522 and *tap-1* backgrounds as described previously (Xie *et al.*, 2015). Sequencing of mutant lines was performed by the Beijing Genomics Institute (BGI). The target sequences used for the CRISPR constructs are listed in Table S1.

Rice was grown in the paddy fields in Shanghai during summer (27–41°C, as high temperature/HT) and in Sanya during winter (14–29°C, as low temperature/LT). Panicles and spikelets used for plant phenotyping were collected from plants grown in growth chambers with controlled photoperiod and temperature treatments (Conviron, GR48, Canada) as follows: rice seedlings were grown under standard growth conditions (average temperature 28°C, 14 h : 10 h, day : night photoperiod) for 1 month and then changed to short-day (SD) conditions (28°C, 11 h : 13 h, day : night photoperiod) for 2 wk to induce the transition from vegetative to reproductive growth. After entering the reproductive phase, rice plants were transferred to growth chambers with an average temperature of 22, 30, or 34°C under LD (14 h : 10 h) or SD (11 h : 13 h) day : night cycles. Detailed settings for growth chambers are provided in Table S2.

To generate complementation line, the *proTAP::TAP–eGFP* construct was created by inserting the full-length fragment of *TAP* gDNA (containing 4231-base-pair promoter) with enhanced green fluorescent protein (eGFP) into the *Eco*RI and *Bst*EII sites of pCAMBIA1301, using In-Fusion (TaKaRa, Kusatsu, Japan) cloning technology, and the constructed vector was introduced into *tap-1* calli using the *Agrobacterium*-mediated transformation method (Hiei *et al.*, 1994).

Characterization of the mutant phenotypes

Images of rice plants and panicles were captured with a Nikon E995 digital camera (Tokyo, Japan). Images of spikelets and floral organs were photographed with a Leica M205A microscope (Wetzlar, Germany). Scanning electron microscopy and

longitudinal section analysis were performed as described previously (Yun *et al.*, 2013).

Map-based cloning

An F_2 mapping population was created from a cross between the *tap-1* mutant and the *Oryza sativa* ssp. *indica* cultivar Guangluai 4, from which 540 mutants were selected for map-based cloning of *TAP*. By fine mapping, the mutation was narrowed down to a region on chromosome 2 between two InDel makers, Y1 and Y8. High-throughput sequencing of the genes between Y1 and Y8 revealed a mutation in *LOC_Os02g18370*. Primers used in the fine mapping are listed in Table S1.

Subcellular localization analysis in rice protoplasts

The *TAP* coding region was cloned into a modified pGreenII 0000 vector between a *35 S* promoter and a sequence encoding GFP using In-Fusion (TaKaRa) cloning technology. The *35 S::TAP-GFP* plasmid and control *35 S::GFP* plasmid were separately transfected into rice protoplasts as described previously (Zhang *et al.*, 2011). After incubation for 12 h at 25°C, the protoplasts were examined using a confocal microscope (Leica SP5). For nuclear staining, the DAPI stock solution was diluted to 300 nM in PBS buffer and then added to the W5 solution with protoplasts for 10 min.

RT-qPCR analysis and *in situ* hybridization

Total RNA was isolated using Trizol reagent (Invitrogen) from roots, 3-wk-old leaves, and young panicles (inflorescences) of different lengths (1–10 mm) from three biological replicates. The Prime Script RT reagent kit with genomic DNA eraser (TaKaRa) was used to synthesize cDNA according to the manufacturer's instructions. qPCR was performed using gene-specific primers (Table S2) using three technical repeats for each biological replicate. The *OsActin1* gene was used as an internal control to normalize transcript levels.

In situ hybridization was performed as described previously (Yun *et al.*, 2013). *TAP* cDNA fragments amplified by PCR (primers listed in Table S1) were used as templates for preparing sense and antisense probes.

ChIP–qPCR

Young panicles 1.5–2.5 mm in length were collected from *tap-1* plants complemented with *proTAP::TAP–eGFP*. The ChIP assay was performed as described by Zhu *et al.* (2022). *OsYAB3/4/5* promoter fragments were quantified by qPCR as described previously (Li *et al.*, 2011), using primers listed in Table S1. Their enrichment in the *proTAP::TAP–eGFP tap-1* samples was compared with levels in wild-type (WT) plants.

Dual-luciferase assays

To create *35 S::TAP-GFP* and *35 S::TDR-GFP* effector vector, the full-length *TAP* and TAPETUM DEGENERATION RETARDATION (TDR) (Fu *et al.*, 2014) cDNA were cloned into modified *pGreenII-0000* vector (*pGreenII-GFP*). The empty vector (*35 S::GFP*) and *35 S::TDR-GFP* were used as negative controls. The reporter *proOsYAB3::LUC*, *proOsYAB4::LUC*, and *proOsYAB5::LUC* was constructed by cloning partial genomic fragments of *OsYAB3* (−1748 to 3953), *OsYAB4* (−3590 to −1), and *OsYAB5* (−2293 to 2057) into the vector *pGreenII-0800-LUC* to drive luciferase expression, respectively. The LUC transactivation (dual-LUC) assay was performed in *Nicotiana benthamiana* leaves as described previously (Li *et al.*, 2014). LUC and REN activities were measured using the Dual-Luciferase reporter kit (Promega). The LUC/REN ratio was measured in a GloMax 20/20 luminometer (Promega). Six biological replicates were used for each experiment.

Yeast assays

To analyze the transcriptional activity of TAP, the coding sequence of TAP was fused in-frame with the GAL4 DNA-binding domain (GAL4 BD) in the pGBKT7 vector. pGBK-TAP and the empty vector were transformed into yeast strain AH109, respectively.

For the yeast two-hybrid assays, pGADT7 was the prey plasmid and pGBKT7 was the bait plasmid (Clontech, USA). Full-length *TAP* cDNA, and cDNA sequences encoding the N-terminal domain (1–695 amino acids), the C-terminal domain (565–1124 amino acids), the first FAR1 DNA-BD (1–479 amino acids), and the second FAR1 DNA-BD (295–695 amino acids) were amplified by PCR and cloned in-frame with the GAL4 DNA-BD of pGBKT7 to generate the GAL4 DNA-BD constructs. The full-length cDNAs of *OsYAB4* and *OsYAB5* were amplified by PCR and cloned into pGADT7 to fuse with the yeast GAL4 activation domain (AD). The Matchmaker GAL4 two-hybrid system (Clontech, Mountain View, CA, USA) was used according to the manufacturer's instructions, in which protein interaction is evidenced by growth on medium lacking histidine and adenine and blue color when grown in the presence of X-α-gal. Primers used for vector construction are listed in Table S1.

Bimolecular fluorescence complementation assays

OsYAB4 or *OsYAB5* cDNA was fused downstream of the N-terminal region of YFP (1–174 amino acids), and *TAP* cDNA was fused upstream of the C-terminal region of YFP (175–240 amino acids), in the pXY106-nYFP and pXY104-cYFP vectors, respectively (Yu *et al.*, 2008). Constructs were transformed into *Agrobacterium tumefaciens* strain GV3101 and infiltrated into *N. benthamiana* leaves (Li *et al.*, 2014). After infiltration, the tobacco plants were left in the dark at 25°C for 48 h. Fluorescence signals were observed under a confocal microscope (Leica SP5). YFP signal was excited with an argon laser at a wavelength of 515 nm and emission detected at 505–530 nm. All primers used for vector construction are listed in Table S1.

Electrophoretic mobility shift assays

The ChIP assay was performed according to Zhu *et al.* (2022). Full-length *TAP* cDNA was cloned into the pGBKT7 vector

(Clontech) for *in vitro* transcription/translation (TNT T7/SP6 Coupled Wheat Germ Extract System; Promega). The binding reaction contained 25 mM Tris–acetate (pH 7.5), 1 mM DTT, 0.1 mg ml^{-1} BSA, 2 mM MgAc, 20 nM FAM-labeled DNA, and 5 µl of *in vitro* synthesized protein. The binding reaction was performed for 30 min at 25°C before loading on a 7.5% native polyacrylamide gel. FAM-labeled probes were visualized using the FAM channel of a ChemiDoc MP imaging system (Bio-Rad). Primers are listed in Table S1.

Co-immunoprecipitation

Full-length *OsYAB4* and *OsYAB5* cDNAs were fused with the 6 × HA tag from the modified PHB vector to produce OsYAB4 and OsYAB5 recombinant proteins tagged with hemagglutinin (6HA). To produce TAP–^{1st}FAR1–YFP, the coding region of the first FAR1 DNA-BD of TAP (1–479 amino acids) was fused with YFP (which is recognized by anti-GFP antibodies). The fusion constructs were cloned into the pHB vector that contained the double CaMV35S promoter. Proteins were transiently co-expressed in tobacco leaves as described above, in combinations shown in figure legends. Proteins were extracted with ice-cold buffer containing 25 mM Tris–HCl at pH 7.5, 150 mM NaCl, 1 mM EDTA, 10% (v/v) glycerol, 1 mM DTT, 2% (v/v) PVP40, 0.1% (v/v) Tween-20, and the Protease Inhibitor Cocktail (Thermo Scientific, Waltham, MA, USA). After centrifugation at 16 000 rcf for 10 min, 10 µl of the supernatant was saved as 'input', and the remainder was incubated with GFP-Trap Magnetic Agarose (ChromoTek, Munich, Germany) for 3 h at 4°C, and the beads were washed three times with wash buffer (10 mM Tris–HCl at pH 7.5, 150 mM NaCl, 0.5 mM EDTA, 0.005% (v/v) IGEPAL-CA630). Samples were analyzed by immunoblotting using the following commercial antibodies: GFP (G1544, 1 : 5000 dilution; Sigma), hemagglutinin (M20003, 1 : 2000 dilution; Abmart, Berkeley Heights, NJ, USA), goat anti-mouse IgG–horseradish peroxidase (HRP) conjugate (M21001, 1 : 5000 dilution; Abmart), and goat anti-rabbit IgG–HRP conjugate (M21002, 1 : 5000 dilution; Abmart). The primers used for vector construction are listed in Table S1.

RNA-seq analysis

RNA-seq libraries were constructed using young panicles collected from WT and *tap-1* plants grown in the paddy fields in Shanghai (average temperature: 30°C; designated HT) or in Sanya (average temperature: 22°C; designated LT). Total RNA isolation, quality control, and RNA-seq were performed by Shanghai NovelBio Co. The raw sequence reads were mapped to the Michigan State University Rice Genome Annotation Project Release 7. The normalized sequence read counts for each gene were calculated to infer transcript abundance in panicles. DEG analysis was performed, using $\log_2$ fold change of ≥ 1.5 and false discovery rate (FDR) < 0.05. Gene ontology (GO) annotations of the detected DEGs were downloaded from the US National Center for Biotechnology Information (www.ncbi.nlm.nih.gov), UniProt (www.uniprot.org), and GO (www.geneontology.org).

Statistical analysis

Statistical analyses of all bar graphs were performed using GraphPad Prism 8.0.2 (https://www.graphpad.com/scientific-software/prism/). One-way or two-way ANOVA was used to evaluate significant variations. Values of $P < 0.05$ were considered statistically significant. The details about the statistical approaches used can be found in the figures or figure legends. The data are presented as mean ± SD.

Results

Identification of a thermosensitive mutant in panicle and spikelet development

To investigate the molecular mechanisms by which rice plants respond to environmental temperatures during early reproduction, we used an existing mutant library in *Oryza sativa* ssp. *japonica* cv 9522 to screen for panicle and/or spikelet defects at high temperatures (Wang *et al.*, 2006). We identified a mutant *thermosensitive barren panicle* (*tap*) and named the first allele *tap-1*. *tap-1* vegetative plant architecture was indistinguishable from the WT (Fig. S1a,b). At 22°C and 28°C, *tap-1* panicles looked similar to WT (Fig. 1a,b; Table S3), but morphological changes became apparent at higher temperatures. At 30°C, *tap-1* panicles were smaller than WT, with significantly decreased numbers of secondary branches and spikelets (Fig. 1c; Table S3); while at 34°C, *tap-1* plants produced dramatically shortened panicles, no secondary branches, and a greatly reduced number of spikelets (Fig. 1d; Table S3).

Spikelet development in *tap-1* plants was also affected by high ambient temperature. A WT spikelet contains two pairs of sterile glumes (rudimentary glumes and empty glumes) and one floret, comprising a lemma, palea, two lodicules, six stamens, and one carpel (Fig. 1e). *tap-1* spikelets developed normally at 22°C (Fig. 1e), but became increasingly disrupted as temperatures increased (Fig. 1e–h). The developmental defects of *tap-1* spikelets could be categorized into five phenotypic classes (Fig. 2a): type I with a normal palea and lemma; type II with an abnormal palea or lemma; type III with an abnormal palea and lemma; type IV that are tiny and arrest early; and type V that fail to initiate spikelets. In addition, type I, II, and III spikelets exhibited malformed and/or reduced numbers of floral organs, homeotic transformation of floral organs, and ectopic carpel formation (Figs 2b, S1c–f). Type IV spikelets arrested very early in development formed pin-like structures with a cone-shaped apex (Fig. 2c–f). In the WT panicle, lateral spikelet meristems initiate at the axils of hair-like bracts (Fig. 2c,h); however, type V spikelet meristems failed to initiate in these axils (Fig. 2g,i; Table S4). The development of *tap-1* plants was also observed under different day lengths, but changes in photoperiod did not have any obvious effect on panicle and spikelet phenotype (Tables S3, S4), allowing us to conclude that *tap-1* is solely a thermosensitive mutant.

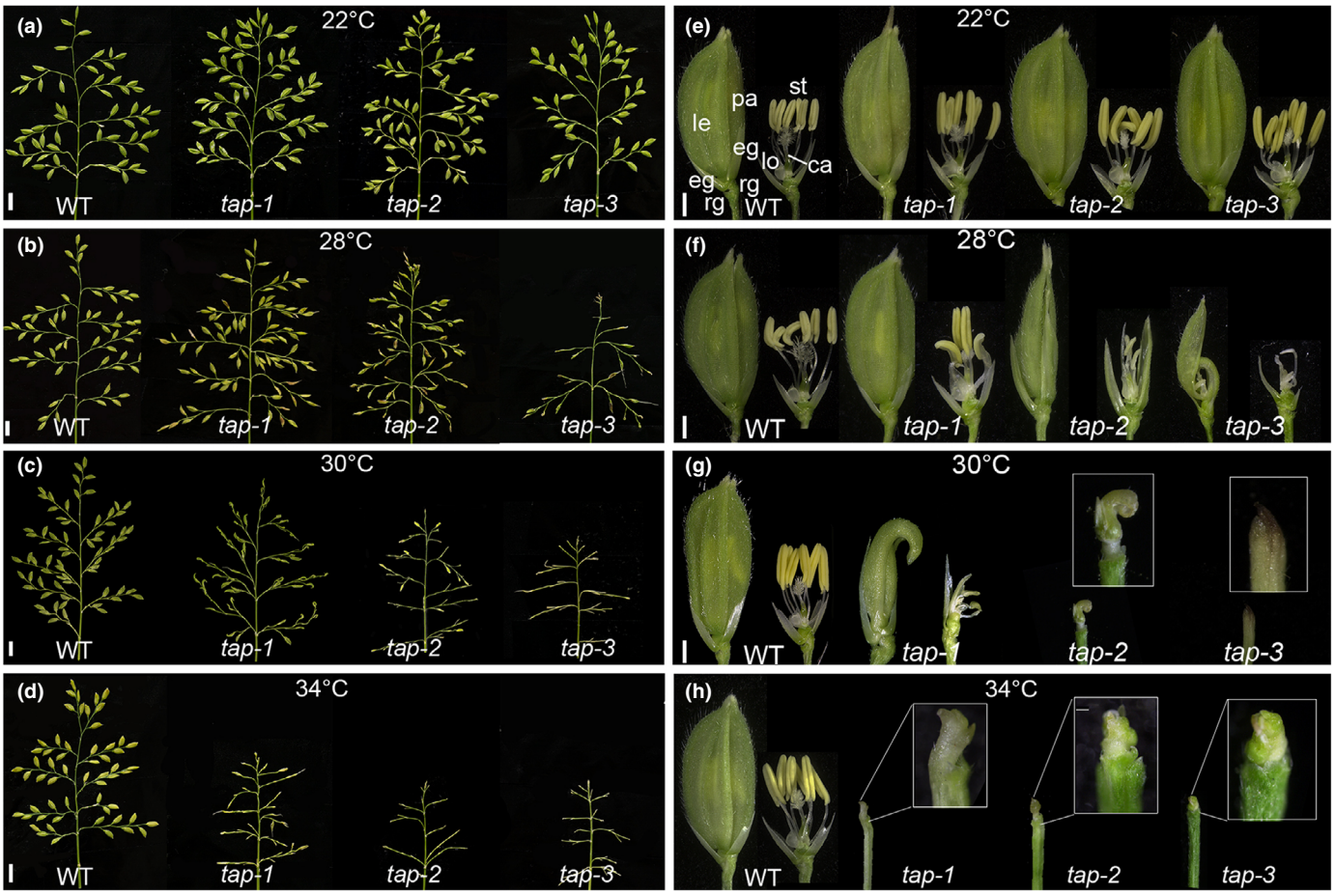

Fig. 1 TAP regulates rice panicle and spikelet development in response to high temperatures. (a–d) Phenotypes of wild-type (WT) and *tap* mutant panicles at various temperatures. Bars, 1 cm. (e–h) Morphology of the WT and the *tap* mutant spikelets at various temperatures. ca, carpel; eg, empty glume; le, lemma; lo, lodicule; pa, palea; rg, rudimentary glume; st, stamen. Bars, 1 mm.

TAP encodes an FRS family transcription factor

To identify the gene responsible for the *tap-1* phenotype, we performed map-based cloning using an F_2 population generated from a cross between *tap-1* and the *indica* cultivar Guangluai 4. The *TAP* locus was mapped to chromosome 2 between two InDel molecular markers, Y1 and Y8 (Fig. 3a). High-throughput sequencing analysis revealed a single base-pair insertion in the last exon of an unannotated gene, LOC_Os02g18370, which resulted in a frameshift and deletion of 89 amino acids from the putative protein (Fig. 3b). To confirm *TAP* as the causative gene underlying the *tap-1* phenotype, we introduced a WT (cv 9522) 8.3 kb genomic fragment containing the upstream regulatory region and the eGFP-tagged coding sequence of LOC_Os02g18370 into the *tap-1* mutant line. The *tap-1* panicle and spikelet defects were completely rescued in the complemented line (Fig. S2), confirming that the single base-pair insertion in *TAP* is the causal mutation for the *tap-1* phenotype.

Protein sequence analysis revealed that TAP contains two N-terminal C2H2 zinc-finger domains (FAR1 DNA-BDs), a central MULE transposase domain, and a C-terminal SWIM zinc-finger domain (Fig. 3b), all of which are FRS family protein characteristics. Transient expression of the TAP-GFP fusion protein in rice protoplasts, driven by the constitutive cauliflower mosaic virus 35 S promoter (pro35S), was used to examine the subcellular localization of TAP, using the empty vector (pro35S::GFP) as control (Fig. 3c). TAP-GFP was observed to overlap well with the nuclear DAPI stain, indicating that TAP is a nucleus-localized protein (Fig. 3c). Next, we used the yeast GAL4 system to evaluate the transcriptional activation activity of the TAP protein (Fig. 3d). The coding sequence of TAP was fused to the GAL4 DNA-BD in the pGBKT7 vector, which lacks the GAL4 AD. TAP was able to activate the expression of downstream reporter genes, indicating that TAP could act as a transcriptional activator. These results demonstrated that, similar to its *Arabidopsis* homolog FAR1 (Lin *et al.*, 2007), TAP is a nuclear transcriptional factor.

TAP is essential for high-temperature response

The mutation in *tap-1* is very close to the end of the coding sequence and leaves all conserved FRS domains intact (Fig. 3b). To further elucidate the function of TAP in temperature response, it was necessary to generate proteins with mutations earlier in the protein sequence. To this end, we used CRISPR/Cas9 technology to disrupt TAP functional domains in two new

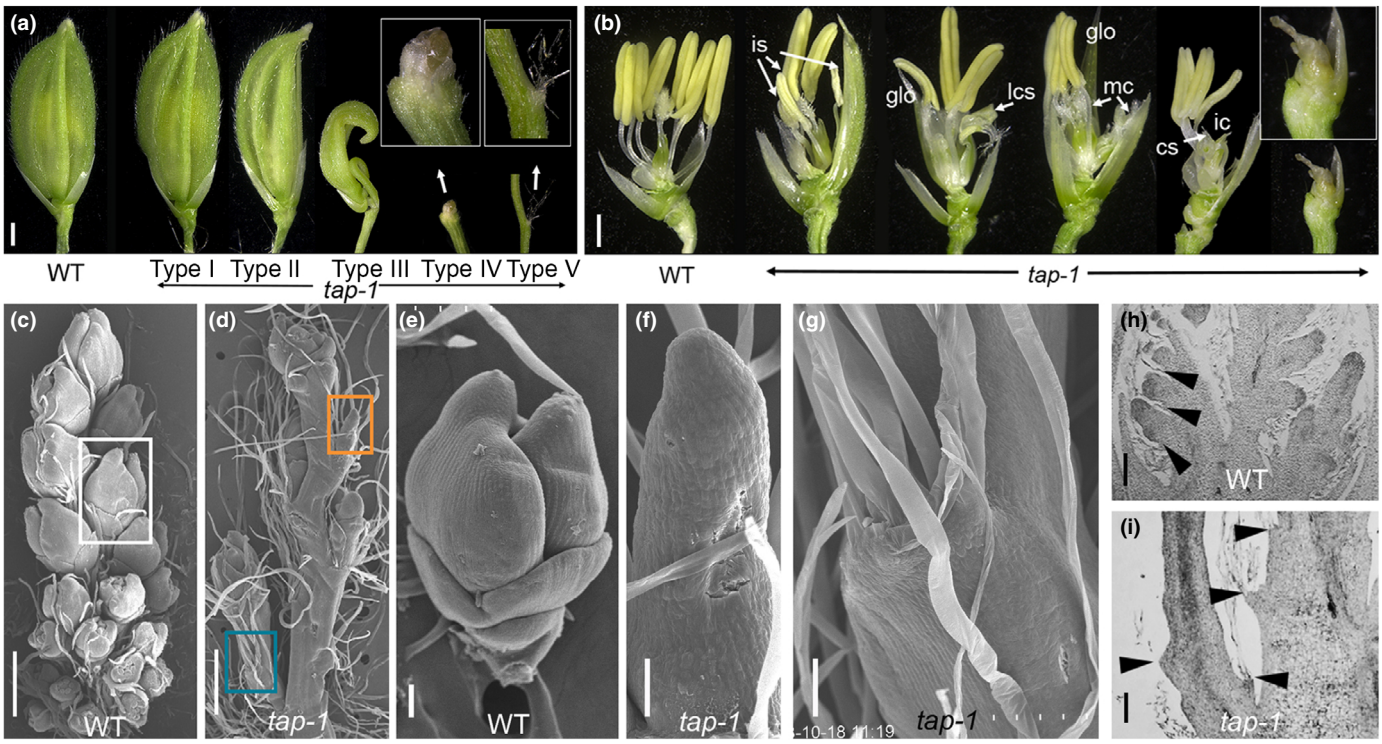

Fig. 2 High temperature disrupts rice spikelet development in *tap-1* mutant. (a) The phenotypic categories of mature *tap-1* spikelets at 30°C, with higher magnification insets of type IV and type V spikelets. (b) Mature *tap-1* flowers at 30°C, with a higher magnification inset of the inner whorls of the stagnant spikelet. cs, carpel–stamen mosaic organ; glo, glume-like lodicule; ic, immature carpel; is, immature stamen; lcs, lodicule–carpel–stamen mosaic organ; mc, multiple carpeloids. (c, d) Scanning electron micrographs of the primary branch of wild-type (WT) (c) and *tap-1* (d) panicles. White, yellow, and cyan boxes indicate a WT, type IV, and type V spikelet, respectively. (e–g) A close-up of the WT spikelet from (c), type IV spikelet from (d), and type V spikelet from (d), respectively. (h, i) Longitudinal section of a developing WT (h) and *tap-1* (i) panicle. Arrowheads indicate axillary hair-like structures. Bars: (a, b) 1 mm; (c, d) 500 μm; (e–g) 50 μm; (h, i) 100 μm.

alleles: *tap-2* and *tap-3* (Fig. 3b). *tap-2* creates a premature translation termination codon before the second FAR1 DNA-BD, while *tap-3* encodes a truncated protein without any of the conserved functional domains.

Similar to *tap-1*, *tap-2* and *tap-3* plants also show thermosensitive defects in panicle and spikelet development under controlled growth conditions (Fig. 1; Tables S3, S4). They grew normally at 22°C and displayed reproductive defects as temperatures increased, with more pronounced phenotypes than *tap-1* lines at the same temperature. At 30°C, *tap-2* panicles produced fewer secondary branches and spikelets than *tap-1* (Fig. 1c; Table S3), and there was no type I and type II spikelets (Table S4). At the same temperature, *tap-3* panicles produced no secondary branches and dramatically less spikelets than any other lines (Fig. 1c; Table S3), with a greatly increased proportion of type IV spikelets (65%; Table S4); in addition, 26% of spikelets were type V, resulting in the formation of naked branches (Fig. 1c). At 34°C, both *tap-2* and *tap-3* panicles lacked secondary branches and only contained type IV and type V spikelets, leading to naked branches (Fig. 1d; Tables S3, S4). These results further support our conclusion that the transcription factor TAP acts as a transducer of the high-temperature signal during panicle and spikelet development in rice, and the severity of the thermosensitive phenotype correlates with the level of TAP protein truncation.

TAP is highly expressed in reproductive organs and induced at high ambient temperatures

Quantitative real-time PCR (RT-qPCR) revealed that *TAP* was preferentially expressed in panicles at early developmental stages, that is, from inflorescence developmental stage 3 (In3) to spikelet developmental stage 8 (Itoh *et al.*, 2005), but at much lower levels in vegetative tissues (Fig. 4a). Using *in situ* hybridization to further examine its spatiotemporal expression, *TAP* was observed to be highly enriched in the meristems of primary and secondary branches and spikelets (Fig. 4b–d). During spikelet organogenesis, *TAP* transcripts were first detected in the regions where the spikelet starts to initiate (Fig. 4d,f), uniformly expressed in the spikelet meristem (Fig. 4g), followed by sequential expression in the primordia of rudimentary and empty glumes (Fig. 4h), the palea and lemma (Fig. 4i), and lodicules and stamens (Fig. 4j). Thus, TAP appears to play a broad role during early reproductive development, from branch initiation to floral organ development.

To further investigate the temperature-dependent nature of the *tap* mutant phenotypes, we compared *TAP* expression in panicles of WT plants grown at high and low temperatures. Plants were grown at 22°C until young panicles reached 2 mm in length, after which half of the plants were transferred to 35°C. An approximately fourfold induction of *TAP* expression was

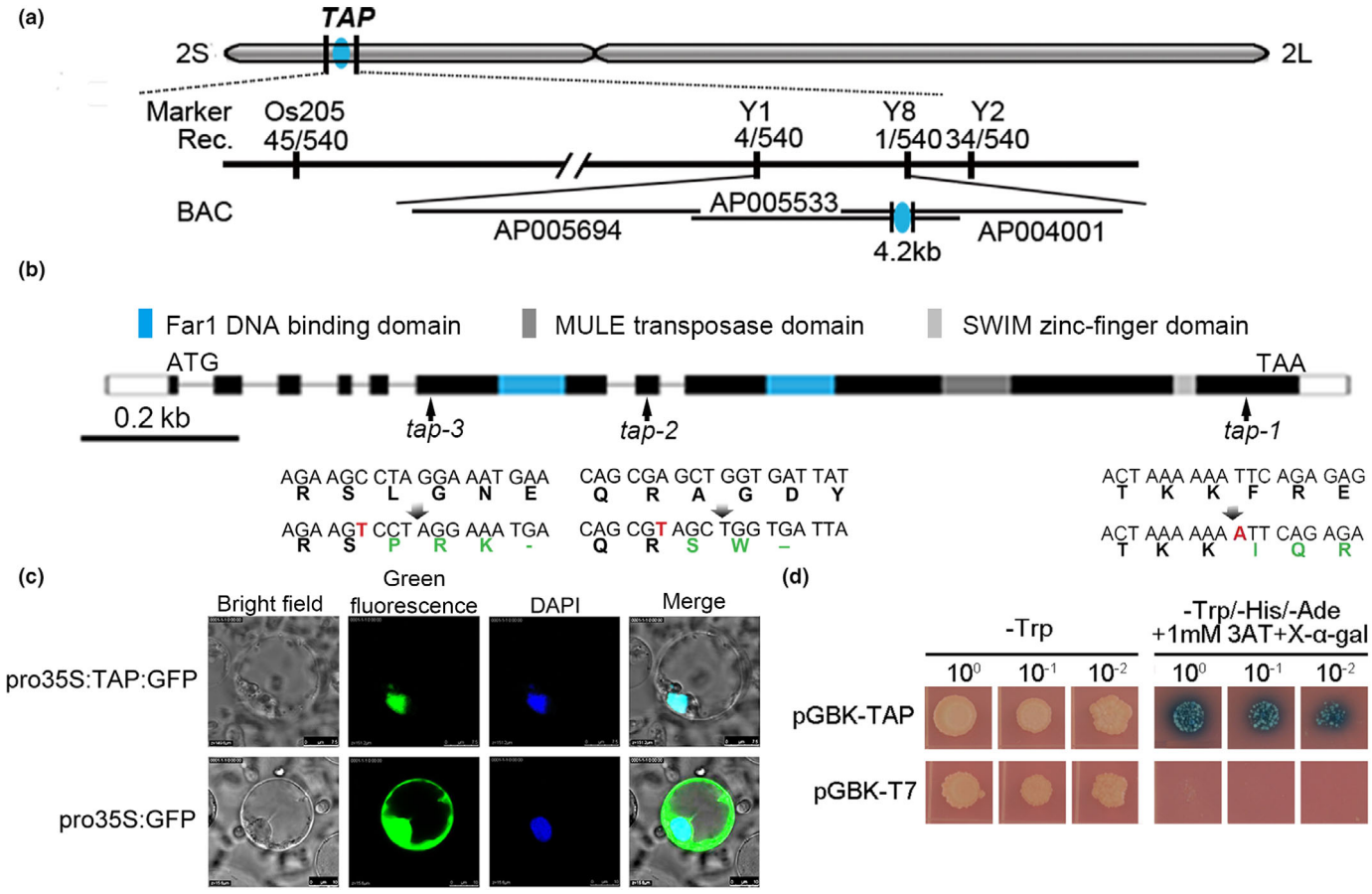

Fig. 3 Cloning and characterization of the rice gene *TAP*. (a) The *TAP* gene is located on BAC clone AP005533 from rice chromosome 2. (b) Schematic representation of the *TAP* gene and encoded protein domains. White boxes represent untranslated regions. Positions of the mutations in the three *tap* alleles are indicated. (c) TAP-GFP is localized in the nucleus, which stains with DAPI. Bars, 7.5 μm. (d) The TAP protein, fused to the GAL4 binding domain in pGBK7, can activate the expression of downstream reporter genes.

observed within 2 h of transfer to the high-temperature condition (Fig. 4k). The longer-term effect on *TAP* expression was examined in 2 mm panicles of WT plants that had grown at 22°C, 30°C, or 35°C for 2 wk, revealing that *TAP* expression became significantly elevated as ambient temperature increased (Fig. 4l). Consistently, an increase in the TAP protein abundance was observed under the same conditions (Fig. 4m).

TAP is a key regulator of panicle and spikelet development

To elucidate the regulatory role of TAP in panicle and spikelet development, we used RNA-sequencing (RNA-seq) analysis to identify differentially expressed genes (DEGs) in *tap-1* panicles. RNA-seq libraries were constructed using young panicles collected from WT and *tap-1* plants grown at 30°C (HT) or 22°C (LT). Samples were collected from two developmental stages: the start of secondary branch initiation and differentiation (panicles 1.5–2 mm; stage 1); and the completion of spikelet differentiation (panicles 2.5–3 mm; stage 2). RNA-seq analysis identified 1190 DEGs from stage 1 and 1478 DEGs from stage 2 at HT (Fig. 5a), which decreased to 537 at stage 1 and 391 at stage 2 at LT (Fig. 5b).

Gene ontology enrichment analysis on overlapping DEGs between the two stages at HT identified that upregulated DEGs were mainly enriched in processes such as general catabolism, stress response, and light harvesting (Table S5), while downregulated DEGs were mainly enriched in flower and meristem development, transcription, and cell differentiation (Fig. 5c; Table S5). At LT, both the up- and downregulated DEGs were highly enriched in processes such as long-day photoperiodism, flowering, and circadian rhythm (Fig. 5d; Table S6). These data suggest that TAP acts as a key regulator in panicle and spikelet development at high ambient temperature, possibly by regulating the expression of genes involved in related developmental processes.

Given the role of TAP in reproductive development, we focused on DEGs related to flower and meristem development, and cell differentiation (Table S7). From the 226 overlapping and downregulated genes at HT, 13 genes were repeatedly enriched in these GO categories (Fig. 5e). Ten of the 13 were MADS-box transcription factors with a known role in specifying floral organ identity (Sommer *et al.*, 1990; Yanofsky *et al.*, 1990; Saedler *et al.*, 2001), including B-class (*OsMADS4* and *OsMADS16*), C-class (*OsMADS3* and *OsMADS58*), D-class

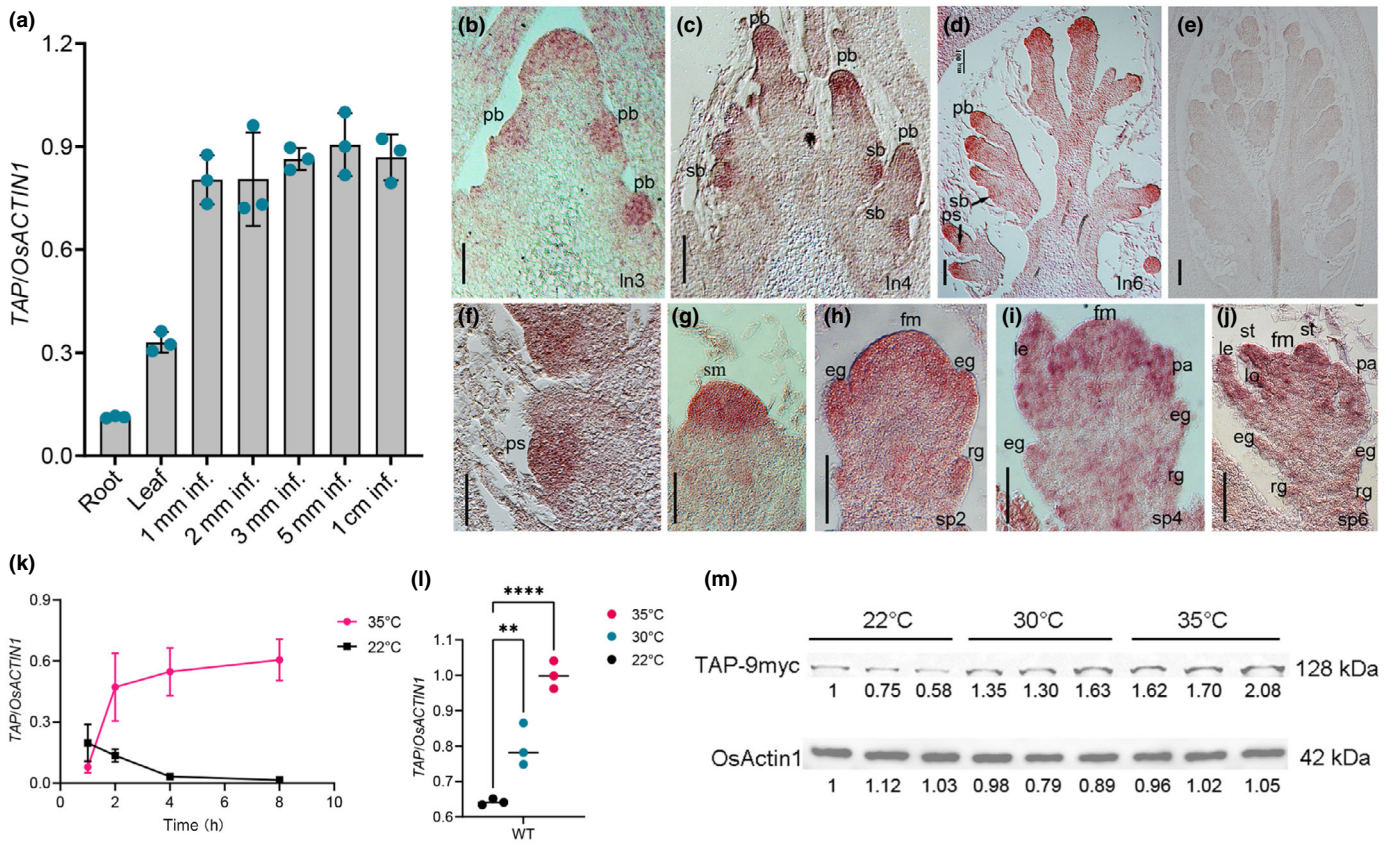

Fig. 4 Expression pattern of the rice gene *TAP*. (a) Relative transcript levels of *TAP* in different rice tissues. inf, inflorescence. (b–e) *In situ* hybridization assay showing *TAP* distribution in young panicles at stages In3 (b), In4 (c), and In6 (d). Control hybridizations with a sense probe showed no signal (e). (f–j) *TAP* mRNA distribution in spikelet development: spikelet primordium (f), spikelet meristem (g), primordium of rudimentary glume (sp2, h), primordium of palea and lemma (sp4, i), and stamen primordium (sp6, j). eg, empty glume; fm, floret meristem; le, lemma; lo, lodicule; pa, palea; pb, primary branch; ps, primordium of spikelet; rg, rudimentary glume; sb, secondary branch; sm, spikelet meristem; st, stamen. Bars: (b–g) 100 μm; (h–j) 50 μm. (k) Time course of *TAP* expression in young panicles (< 2 mm) exposed to different temperatures. (l) *TAP* expression in young panicles (< 2 mm) of plants after 2-wk growth at different temperatures. (m) TAP protein levels in young panicles grown at different temperatures for 2 wk. OsActin1 is used as a loading control. All data are mean ± SD of three biological replicates (cyan dots in a). **, $P < 0.01$; ****, $P < 0.0001$ (pairwise one-way ANOVA).

(*OsMADS13*), and E-class (*OsMADS1*, *OsMADS7*, and *OsMADS8*) genes. The remaining three were *YAB* family genes, including *OsYAB1*, *OsYAB4*, and *DL*, whose orthologs *FIL* and *CRC* play a crucial role in Arabidopsis flower and inflorescence development (Fig. 5e; Tanaka *et al.*, 2012, 2017). These 13 genes were significantly downregulated in *tap-1* compared with WT panicles at HT, but exhibited little, if any, expression changes at LT, consistent with the observed lack of *tap-1* panicle and spikelet defects at LT (Figs 1, 5e). Many of the remaining genes differentially expressed at HT also have reported roles in the regulation of panicle and spikelet development (Table S7), strongly supporting a key role for TAP as a regulator of panicle and spikelet development at high ambient temperature.

TAP interacts with OsYAB4 and OsYAB5 to regulate panicle and spikelet development

Mutant *tap* panicles grown at 34°C resemble those of the *OsYAB3-OsYAB4*-RNAi *osyab5* line (Tanaka *et al.*, 2017). This similarity, together with our RNA-seq results, led us to propose that, at high ambient temperatures, TAP regulates panicle and spikelet development at least partly through the *OsYAB* genes. To test this hypothesis, we compared the expression of *OsYAB3*, *OsYAB4*, and *OsYAB5* in WT and *tap-3* panicles grown at different temperatures (Fig. 6a). All three *OsYAB* genes were significantly downregulated in *tap-3* panicles at high ambient temperatures (30°C and 34°C) but not at 22°C. *Arabidopsis* FRS transcription factors are known to regulate the expression of target genes through *cis*-elements such as CACGCGC (FBS), TGTGTG (FRB1), TATATATATATATATATAT (FRB2), and TATACATA (FRB3) (Ouyang *et al.*, 2011; Ritter *et al.*, 2017), so we analyzed the genomic sequence of *OsYAB3*, *OsYAB4*, and *OsYAB5* and found FRB1 to be predominant in all three *OsYAB* genes, FBS in both *OsYAB4* and *OsYAB5*, and FRB3 only in *OsYAB4*. To determine whether TAP could directly regulate these genes, we performed ChIP–PCR analysis on *tap-1* complemented lines (Fig. 6b). Some genomic fragments from *OsYAB3*, *OsYAB4*, and *OsYAB5* were enriched. In a further dual-luciferase assay, we fused partial genomic fragments (containing promoter regions) from *OsYAB3*, *OsYAB4*, and *OsYAB5* with luciferase coding sequences in reporter constructs (Fig. 6c), and tested whether TAP could regulate *OsYAB3*, *OsYAB4*, and *OsYAB5*

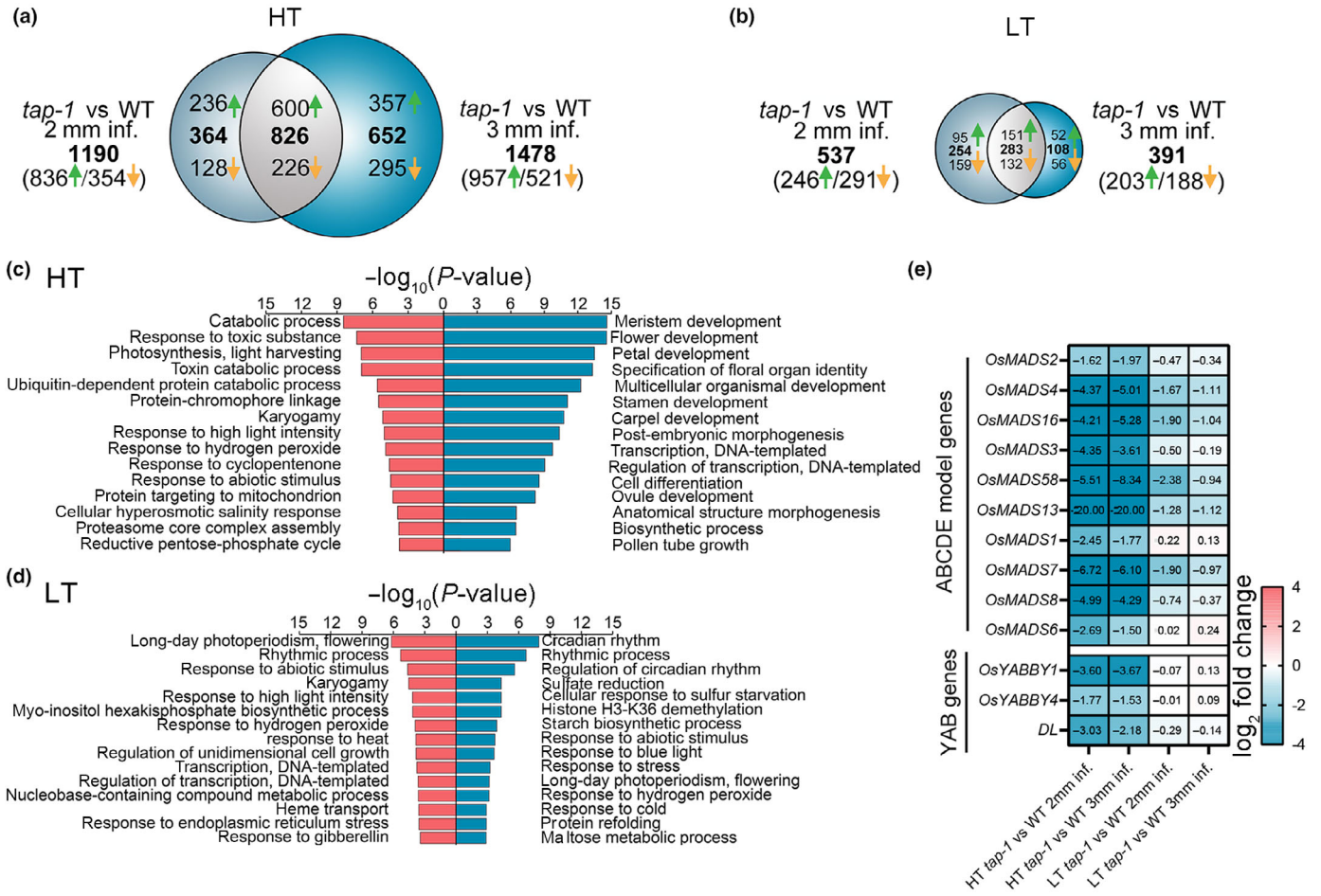

Fig. 5 RNA-seq analysis of the global transcriptome in rice young panicles. (a, b) Venn diagrams showing the total number of differentially expressed genes (DEGs) (log_2 fold change ≥ 1.5 and FDR < 0.05) between *tap-1* and wild-type (WT) panicles at different stages under high (HT) (a) and low (b) (LT) temperature conditions. Green and yellow arrows indicate the number of genes up- and downregulated, respectively, in *tap-1* panicles. Inf, inflorescence. (c, d) Top 15 significant GO terms associated with the upregulated (red) and downregulated (blue) genes from overlapping DEGs in (a) and (b), respectively. (e) Heat map of the genes enriched in meristem development, flower development, and cell differentiation. ABCDE model genes and several *YAB* genes are highlighted. Values indicate log_2 fold changes from the WT.

expression. The results indicated that TAP could directly regulate the expression of *OsYAB3*, *OsYAB4* and *OsYAB5* (Fig. 6c). Electrophoretic mobility shift assays (Fig. 6d) revealed that TAP strongly and preferentially binds to FRB1 motifs in promoters of each *OsYAB* gene (Fig. 6b; Table S2); competition with nonlabeled probes inhibited binding.

Although these results indicated that TAP regulates panicle development via activation of *OsYAB* expression, overexpression of *OsYABs* could not complement *tap* phenotypes (data not shown). To test whether TAP may also act with OsYABs at the protein level, we used yeast two-hybrid assays to show that TAP interacts with OsYAB4 and OsYAB5 (Fig. 7a) via its first FAR1 DNA-BD (Fig. 7b), confirmed by *in vivo* co-immunoprecipitation assays using truncated TAP (Fig. 7c,d). Finally, bimolecular fluorescence complementation (BiFC) assays in *N. benthamiana* confirmed protein–protein interactions between TAP and OsYAB4/OsYAB5 (Fig. 7e,f). Thus, TAP interplays with the OsYAB function both at the transcript and protein levels during panicle and spikelet development by upregulating expression of *OsYAB3/4/5* and physically interacting with OsYAB4 and OsYAB5.

To study the biological function of the TAP–OsYAB4/5 complex, we used CRISPR/Cas9 in WT and *tap-1* backgrounds to create individual and multiple loss-of-function mutants of *OsYAB4* and *OsYAB5* (Figs S3–S5). At 28°C, neither of the *osyab4* or *osyab5* single mutants in the WT background displayed obvious changes in panicle architecture (Fig. S4c,f), but some spikelets showed pleotropic defects. In *osyab4*. impaired palea, glume-like lodicules, decreased number of stamens, and multiple carpels were observed in *c.* 9% of spikelets (Fig. S4e). In *osyab5*, 31% of spikelets had an elongated awn; 7% formed an impaired cone-shaped organ without margins and lost their inner flower organs; 14% developed extra lemma/palea-like organs; and 9% showed striking similarity with type III spikelets found in *tap* mutants (Fig. S4h). The *osyab4* or *osyab5* single mutants in the *tap-1* background caused synergistic developmental defects, including smaller panicles (Fig. S4d,g), and the ratio of abnormal florets increased significantly in both (Fig. S4e,i). In *osyab4 tap-1*

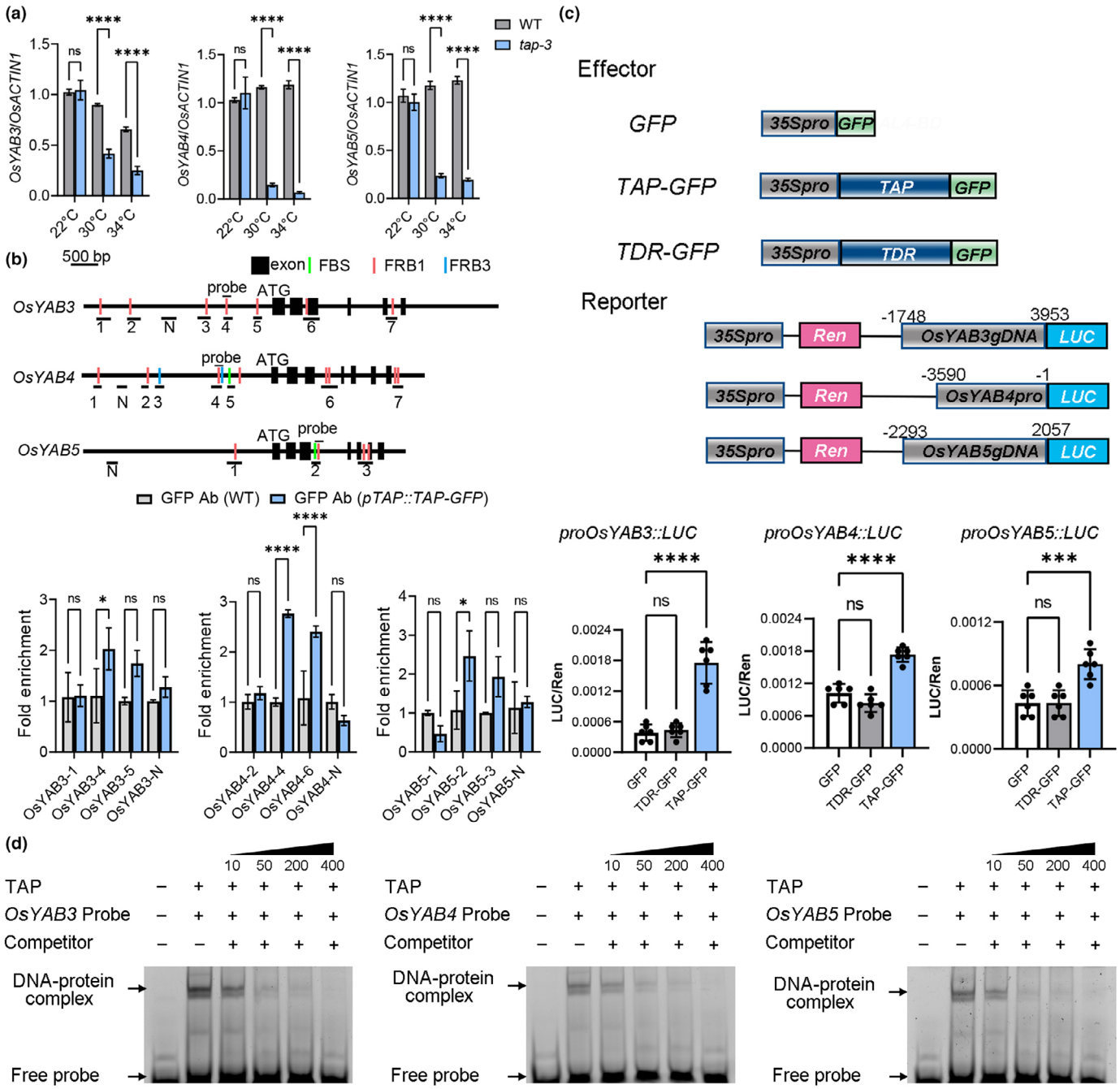

Fig. 6 TAP directly regulates rice *OsYAB* transcription. (a) Relative *OsYAB3*, *OsYAB4*, and *OsYAB5* expression in wild-type (WT) and *tap-3* panicles (Sp4–Sp6) at different temperatures. Data are mean ± SD of three biological replicates. ***, $P < 0.001$ (pairwise two-way ANOVA). (b) ChIP–qPCR enrichment of regulatory regions in *OsYAB3*, *OsYAB4*, and *OsYAB5* genes in *proTAP::TAP–eGFP tap-1* transgenic plants compared with WT plants at high temperature. Various motifs in the promoter or introns are indicated. The locations of probe used in the electrophoretic mobility shift assay (EMSA) are indicated. Data are mean ± SD of three independent experiments. *, $P < 0.05$; ****, $P < 0.0001$; ns, not significant (pairwise one-way ANOVA). (c) Transient expression assay in tobacco. *pro35S::GFP*, *pro35S::TAP-GFP* and *pro35S::TDR-GFP* were cotransformed with *proOsYAB3::LUC*, *proOsYAB4::LUC*, and *proOsYAB5::LUC* into *Nicotiana benthamiana*, respectively. *TDR* (*Tapetum Degeneration Retardation*) encodes a nuclear protein, used as negative control. Data are mean ± SD of six independent experiments. ***, $P < 0.001$; ****, $P < 0.0001$; ns, not significant (pairwise two-way ANOVA). (d) EMSA using TAP and the *OsYAB3/4/5* promoter sequences containing FRB1 *cis*-regulatory elements. Competition binding assays of TAP to *OsYAB3*, *OsYAB4*, and *OsYAB5* probe labeled with 5′-FAM was carried out with unlabeled probe at 10, 50, 200 or 400× concentration of labeled probe.

lines, 27% of spikelets had an elongated awn and 30% type III–like spikelets were observed, which were not found in either *osyab4* or *tap-1* single mutant lines (Fig. S4e). In *osyab5 tap-1* lines, the growth of the lemma and palea was suppressed in 93% of spikelets, such that they were unable to enclose the inner floral organs and the development of the inner flower organs was arrested (Fig. S4i). Finally, the loss of *OsYAB4* and *OsYAB5* function simultaneously in WT plants generated panicles that only

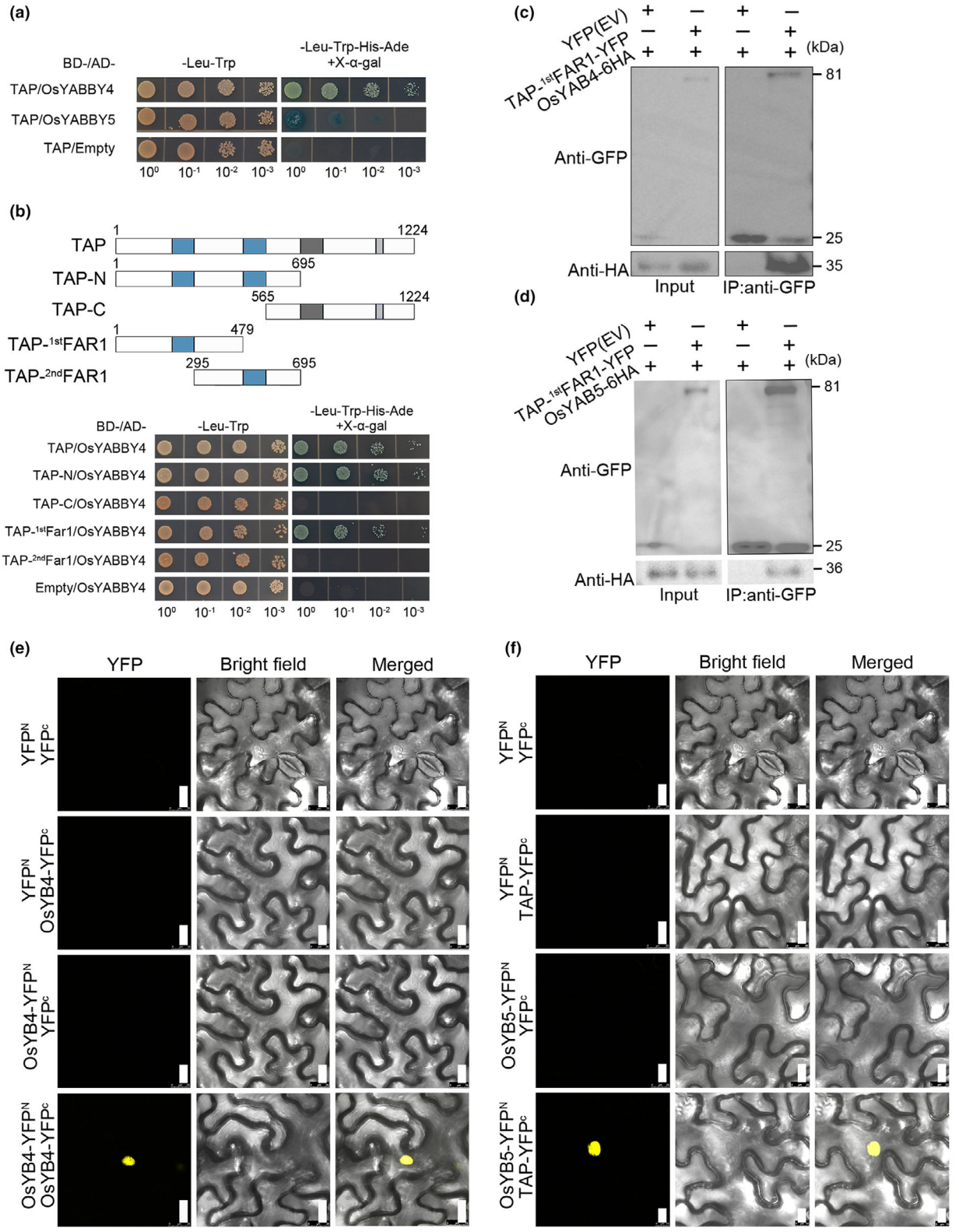

Fig. 7 TAP interacts with OsYAB4 and OsYAB5 in rice. (a) Yeast two-hybrid assays showing that TAP interacts with OsYAB4 and OsYAB5. Empty vector pGADT7 was used as the negative control. BD, binding domain; AD, activation domain. Growth on nonselective (left) and selective (right) media. (b) TAP interacts with OsYAB4 through its first FAR1 DNA-binding domain. FAR1 domains, blue boxes; MULE transposase domain, dark gray boxes; SWIM zinc-finger domain, light gray boxes. (c, d) Co-immunoprecipitation (IP) assays of tobacco leaf extracts transiently expressing TAP–^{1st}FAR1–YFP with OsYAB4 (c) or OsYAB5 (d). (e, f) Bimolecular fluorescence complementation (BiFC) confirming the physical interaction between TAP and OsYAB4 (e) or OsYAB5 (f) in *Nicotiana benthamiana*. Bars, 25 μm.

had naked branches (Fig. S4j), as observed in *tap* mutants at high ambient temperature. In the *tap-1* background, the *osyab4* or *osyab5* double mutation increased the proportion of type V spikelets compared with the *osyab4 osyab5* double mutant in the WT background (Fig. S4l,m).

At 34°C, *osyab4* spikelets showed a stronger phenotype than at 28°C, and the proportion of different *osyab5* spikelet mutations also changed (cf Fig. S5 with Fig. S4), indicating that *osyab4* and *osyab5* single mutants are also sensitive to temperature. The *osyab4 tap-1* and *osyab5 tap-1* panicles were similar to *tap-1* panicles (Fig. S5b,d,g), while a higher proportion of *osyab tap* spikelets failed to initiate or develop (25% in *osyab4 tap-1*, 36% in *osyab5 tap-1* compared with 12% in *tap-1*; Fig. S5e,i), a trend also observed with the double *osyab* mutant (77% in *osyab4 osyab5* vs 89% in *osyab4 osyab5 tap-1*; Fig. S5l,m). These results indicate that TAP, OsYAB4, and OsYAB5 work together to control panicle and spikelet development in response to plant growth temperature.

Discussion

According to the Food and Agriculture Organization report, *The State of Food Security and Nutrition in the World 2020*, extreme climate events, including high temperature, will increasingly become the 'new normal' (Bongaarts, 2021), posing new challenges to food security. Understanding the heat-adaptive mechanisms of plants is of utmost importance for breeding new crop varieties with enhanced resilience to temperature stresses. Here, we report a new thermosensitive transcription factor, TAP, which belongs to the transposase-derived FRS family of proteins, and is essential to maintain normal reproductive growth in rice at high ambient temperatures.

During rice panicle initiation, the development of secondary branches and the attached florets is highly vulnerable to high temperature stress (Wu *et al.*, 2019). Interestingly, defects in reproductive development of *tap* mutants only emerge at high ambient temperatures and affect panicle secondary branch and spikelet development (Fig. 1; Tables S3, S4). The induction of *TAP* transcription in response to high temperature (Fig. 4k,l) may represent an acclimation mechanism of rice plants to heat stress. We predict that the domestication of *TAP* in rice may correlate with the adaption of rice plants to changing environmental temperatures.

Evidence is accumulating that the molecular domestication of transposable elements has served to meet the challenges of the changing environment (Miller *et al.*, 2000; Lin *et al.*, 2007). *Mutator* and *Mutator-like* transposable elements (MULEs) and their derived chimeric genes are widespread in grass genomes. In *Arabidopsis*, domestication of the *Mutator* transposase-derived *FAR1* and *FHY3* genes, which play critical roles in light signal transduction, was closely associated with the far-red light response (Lin *et al.*, 2007). In a recent phylogenetic study, *TAP* was shown to cluster with a *Poaceae*-specific subgroup (G25) of the *FAR* superfamily, distantly associated with the dicot subgroups containing *FAR1* and *FHY3* (Young Chae *et al.*, 2021).

In *Arabidopsis*, the FRS protein FHY3 mediates shoot and floral meristem development in response to light via a complex regulatory pathway involving phytohormones and *CLAVATA* (*CLV*) gene expression (Li *et al.*, 2016). Our study has revealed that the FRS protein TAP controls rice reproductive meristem activity in response to temperature changes. At high ambient temperatures, *tap* mutations cause a plethora of defects in meristem activities, including failure to initiate branch and spikelet meristems, arrest of floral organogenesis, and the partial loss of spikelet meristem indeterminacy (Figs 2, S1). These findings suggest that TAP is required for the function of reproductive meristems as well as floral organ generation at high temperatures. Our results, together with previous studies on FHY3 and FAR1, indicate that FRS family proteins may play evolutionarily conserved roles in plant meristems to integrate environmental signals and developmental cues. It remains to be determined whether temperature-regulated *Arabidopsis* FRS proteins exist, or whether this feature is unique to rice/cereals.

The *Arabidopsis* FHY3 protein directly activates the E-class MADS-box gene *SEPALLATA2* (*SEP2*) (Liu *et al.*, 2016). We have demonstrated that the *tap* mutation causes the downregulation of 10 *OsMADS* genes and three *YAB* genes (Fig. 5e). The FIL/YAB3 subclade of YAB proteins, to which OsYAB3, 4, and 5 belong, play conserved roles in maintaining the proper function of meristems, with distinct distribution patterns in different species (Siegfried *et al.*, 1999; Juarez *et al.*, 2004; Tanaka *et al.*, 2017). *TAP* and *OsYAB3/4/5* share overlapping expression patterns in reproductive organs and similar mutant phenotypes (Fig. 4; Tanaka *et al.*, 2017), and the reduction of *OsYABBY3/4/5* expression in *tap* mutants is positively correlated with the magnitude of temperature increase (Fig. 6a). The TAP protein was shown to act in concert with OsYAB transcription factors to regulate meristem activity at high ambient temperatures, both at the transcriptional level to induce *OsYAB3/4/5* expression, and at the protein level through physical interaction with OsYAB4 and OsYAB5 (Figs 6, 7). These results suggest that TAP and OsYABs may form protein complexes to regulate the expression of genes required for rice reproductive development under heat stress.

Our study has revealed that TAP and OsYAB4/5 constitute a complicated regulatory mechanism. TAP forms protein complexes with OsYAB4 and OsYAB5 to regulate downstream genes, which are critical for panicle and spikelet development; meanwhile TAP directly regulates *OsYAB4* and *OsYAB5* expression, suggesting an autoregulation mechanism (Fig. 8). Similar mechanisms have been reported in the regulation of Arabidopsis floral organogenesis, where the MADS-box protein SEPALLATA3 (SEP3) acts as the 'glue' to stabilize higher-order MADS-box complexes with other floral organ identity regulators, such as AGAMOUS (AG) and APETALA3 (AP3; Causier *et al.*, 2010). Furthermore, SEP3 regulates the expression of these genes via binding to the CArG box elements in their promoters (Kaufmann *et al.*, 2009). Our results suggest that TAP may function as a hub, like SEP3, that integrates developmental and environmental signals during panicle development.

While *OsYAB4*/*OsYAB5* expression does not appear to be heat-sensitive (Fig. 6a), single *osyab4* or *osyab5* mutants exhibited

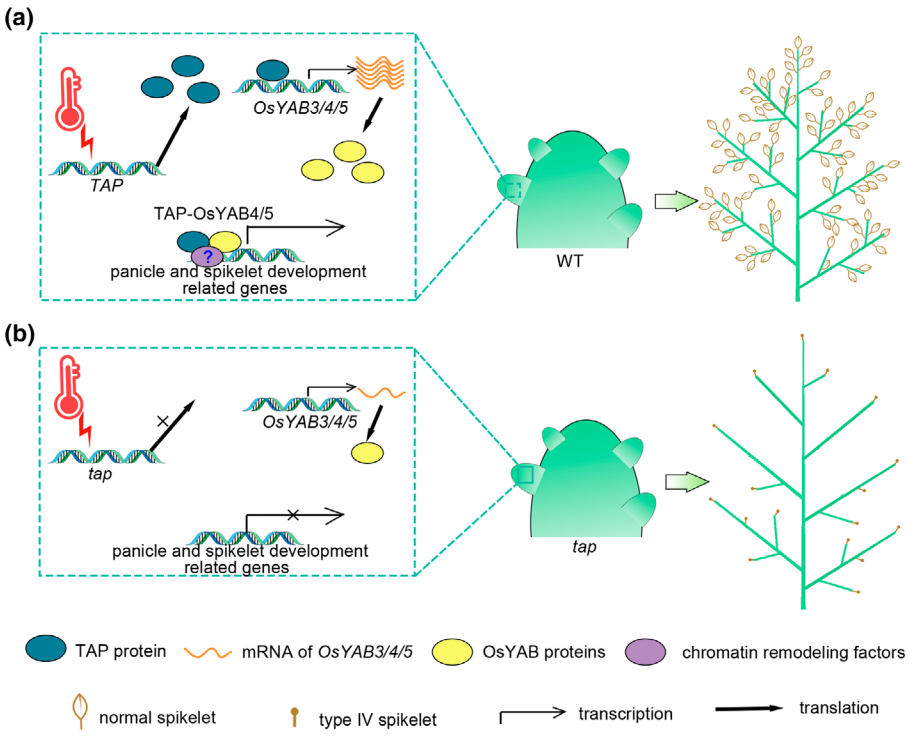

Fig. 8 Proposed model of TAP-mediated rice panicle and spikelet development at high ambient temperatures. (a) In the wild-type (WT), high ambient temperatures increase the abundance of TAP, which directly promotes the expression of the OsYAB3/4/5 genes, then TAP interacts with OsYAB4/5 and may further recruit chromatin remodeling factors to regulate the expression of downstream genes, which are critical for panicle and spikelet development. (b) Disruption of *TAP* leads to reduced levels of *OsYAB3/4/5* expression and disappearance of TAP-OsYAB4/5 complexes, eventually resulting in altered panicle and spikelet development.

temperature-sensitive phenotypic defects (Figs S4, S5). The *tob1* (*osyab5*) mutant phenotype has previously been shown to be affected by environmental factors, with the proportion of different phenotypic classes exhibited varying between seasons and culture conditions (Tanaka *et al.*, 2012). In *Arabidopsis*, activation of *FIL* in the floral organ primordia requires the action of chromatin remodeling factors (Chung *et al.*, 2019). It is likely that TAP and OsYABs are involved in recruiting chromatin remodeling factors to change chromatin conformation, a process that is sensitive to temperature change; the *fil* mutant shows defects in tertiary lateral shoot formation at low temperatures (16°C) (Sawa *et al.*, 1999). *tap* mutants did not display obvious growth defects under normal conditions (average temperature 22–28°C), suggesting that *TAP* is specifically required for growth control at high ambient temperatures. Other factors may also play redundant roles under normal conditions, for example, other members of the rice FRS family. Alternatively, a higher dose of TAP proteins (Fig. 4m) may be required at high ambient temperatures to form a higher-order transcription regulation complex with other factors, such as chromatin remodeling factors or transcription cofactors (Fig. 8). The possible link between the TAP–OsYAB4/5 regulatory network and chromatin remodeling–mediated thermosensitive transcription awaits future investigation.

In summary, we have discovered a pivotal role for the transposase-derived transcription factor TAP in maintaining proper reproductive meristem function under high ambient temperature in rice. Our findings shed light on the molecular mechanisms underlying heat adaptation of cereal crops, which may benefit agricultural efforts to improve crop performance in the face of global environmental change.

Accession numbers

Sequence data from this article can be found in the GenBank/EMBL data libraries under the following accession nos.: *TAP* (Os02g0284500), *OsYAB3* (Os10g0508300), *OsYAB4* (Os02g0643200), *OsYAB5* (Os04g0536300).

Acknowledgements

We thank Zhijin Luo, Mingjiao Chen, and Zibo Chen (Shanghai Jiao Tong University) for mutant screening and generation of F2 populations for mapping. This work was supported by funds from the National Natural Science Foundation of China (U19A2031), the Royal Society (CHL\R1\180496 – Challenge-led Grants 2018), and the Special Funds for Construction of Innovative Provinces in Hunan Province, Programme of Introducing Talents of Discipline to Universities (B14016).

Competing interests

None declared.

Author contributions

WL and DZ designed the project. PZ, WZ, YH, JS, JF, RF and LL performed the experiments. PZ, WL and JH wrote the paper.

ORCID

Yi He https://orcid.org/0000-0002-5218-541X
Jianping Hu https://orcid.org/0000-0002-4635-4299

Wanqi Liang https://orcid.org/0000-0002-9938-5793
Dabing Zhang https://orcid.org/0000-0003-3181-9812
Peng Zhang https://orcid.org/0000-0001-6064-7146
Wanwan Zhu https://orcid.org/0000-0002-3545-0090

Data availability

The raw data files for the RNA-seq analysis reported in this paper have been deposited in the GEO database (accession no. GSE212443). All other data supporting the findings of this study are available within the paper and its Supporting Information files.

References

Allen T, Koustenis A, Theodorou G, Somers DE, Kay SA, Whitelam GC, Devlin PF. 2006. *Arabidopsis* FHY3 specifically gates phytochrome signaling to the circadian clock. *Plant Cell* **18**: 2506–2516.

Bongaarts J. 2021. FAO, IFAD, UNICEF, WFP and WHO. The State of Food Security and Nutrition in the World 2020. Transforming food systems for affordable healthy diets FAO, 2020, 320 p. *Population and Development Review* **47**: 558.

Bowman JL, Smyth DR. 1999. CRABS CLAW, a gene that regulates carpel and nectary development in Arabidopsis, encodes a novel protein with zinc finger and helix–loop–helix domains. *Development* **126**: 2387–2396.

Cao Y-Y, Duan H, Yang L-N, Wang Z-Q, Liu L-J, Yang J-C. 2009. Effect of high temperature during heading and early filling on grain yield and physiological characteristics in indica rice. *Acta Agronomica Sinica* **35**: 512–521.

Causier B, Schwarz-Sommer Z, Davies B. 2010. Floral organ identity: 20 years of ABCs. *Seminars in Cell & Developmental Biology* **21**: 73–79.

Chang N, Gao Y, Zhao L, Liu X, Gao H. 2015. *Arabidopsis FHY3/CPD45* regulates far-red light signaling and chloroplast division in parallel. *Scientific Reports* **5**: 9612.

Chen Q, Atkinson A, Otsuga D, Christensen T, Reynolds L, Drews GN. 1999. The Arabidopsis FILAMENTOUS FLOWER gene is required for flower formation. *Development* **126**: 2715–2726.

Chung Y, Zhu Y, Wu M-F, Simonini S, Kuhn A, Armenta-Medina A, Jin R, Østergaard L, Gillmor CS, Wagner D. 2019. Auxin response factors promote organogenesis by chromatin-mediated repression of the pluripotency gene *SHOOTMERISTEMLESS*. *Nature Communications* **10**: 886.

Fedoroff NV. 2012. Transposable elements, epigenetics, and genome evolution. *Science* **338**: 758–767.

Fu Z, Yu J, Cheng X, Zong X, Xu J, Chen M, Li Z, Zhang D, Liang W. 2014. The rice basic helix–loop–helix transcription factor TDR INTERACTING PROTEIN2 is a central switch in early anther development. *Plant Cell* **26**: 1512–1524.

Hiei Y, Ohta S, Komari T, Kumashiro T. 1994. Efficient transformation of rice (*Oryza sativa* L.) mediated by Agrobacterium and sequence analysis of the boundaries of the T-DNA. *The Plant Journal* **6**: 271–282.

Hudson M, Ringli C, Boylan MT, Quail PH. 1999. The FAR1 locus encodes a novel nuclear protein specific to phytochrome A signaling. *Genes & Development* **13**: 2017–2027.

Hudson ME, Lisch DR, Quail PH. 2003. The FHY3 and FAR1 genes encode transposase-related proteins involved in regulation of gene expression by the phytochrome A-signaling pathway. *The Plant Journal* **34**: 453–471.

Ikeda K, Sunohara H, Nagato Y. 2004. Developmental course of inflorescence and spikelet in rice. *Breeding Science* **54**: 147–156.

Itoh J-I, Nonomura K-I, Ikeda K, Yamaki S, Inukai Y, Yamagishi H, Kitano H, Nagato Y. 2005. Rice plant development: from zygote to spikelet. *Plant and Cell Physiology* **46**: 23–47.

Jacott CN, Boden SA. 2020. Feeling the heat: developmental and molecular responses of wheat and barley to high ambient temperatures. *Journal of Experimental Botany* **71**: 5740–5751.

Juarez MT, Twigg RW, Timmermans MCP. 2004. Specification of adaxial cell fate during maize leaf development. *Development* **131**: 4533–4544.

Kaufmann K, Muiño JM, Jauregui R, Airoldi CA, Smaczniak C, Krajewski P, Angenent GC. 2009. Target genes of the MADS transcription factor SEPALLATA3: integration of developmental and hormonal pathways in the Arabidopsis flower. *PLoS Biology* **7**: e1000090.

Li D, Fu X, Guo L, Huang Z, Li Y, Liu Y, He Z, Cao X, Ma X, Zhao M *et al.* 2016. *FAR-RED ELONGATED HYPOCOTYL3* activates *SEPALLATA2* but inhibits *CLAVATA3* to regulate meristem determinacy and maintenance in *Arabidopsis*. *Proceedings of the National Academy of Sciences, USA* **113**: 9375–9380.

Li G, Kuijer HNJ, Yang X, Liu H, Shen C, Shi J, Betts N, Tucker MR, Liang W, Waugh R *et al.* 2021. MADS1 maintains barley spike morphology at high ambient temperatures. *Nature Plants* **7**: 1093–1107.

Li G, Liang W, Zhang X, Ren H, Hu J, Bennett MJ, Zhang D. 2014. Rice actin-binding protein RMD is a key link in the auxin–actin regulatory loop that controls cell growth. *Proceedings of the National Academy of Sciences, USA* **111**: 10377–10382.

Li G, Siddiqui H, Teng Y, Lin R, Wan X, Li J, Lau O-S, Ouyang X, Dai M, Wan J *et al.* 2011. Coordinated transcriptional regulation underlying the circadian clock in Arabidopsis. *Nature Cell Biology* **13**: 616–622.

Lin R, Ding L, Casola C, Ripoll DR, Feschotte C, Wang H. 2007. Transposase-derived transcription factors regulate light signaling in *Arabidopsis*. *Science* **318**: 1302–1305.

Liu L, Li B, Liu X. 2016. *FAR-RED ELONGATED HYPOCOTYL3* promotes floral meristem determinacy in Arabidopsis. *Plant Signaling & Behavior* **11**: e1238545.

Miller WJ, McDonald JF, Nouaud D, Anxolabéhère D. 2000. Molecular domestication – more than a sporadic episode in evolution. In: McDonald JF, ed. *Transposable elements and genome evolution*. Dordrecht, the Netherlands: Springer Netherlands, 197–207.

Ouyang X, Li J, Li G, Li B, Chen B, Shen H, Huang X, Mo X, Wan X, Lin R *et al.* 2011. Genome-wide binding site analysis of FAR-RED ELONGATED HYPOCOTYL3 reveals its novel function in *Arabidopsis* development. *Plant Cell* **23**: 2514–2535.

Palermo BRZ, Dornelas MC. 2021. Beyond YABBYs: a focus on versatility and interactivity. *Tropical Plant Biology* **14**: 213–225.

Ritter A, Iñigo S, Fernández-Calvo P, Heyndrickx KS, Dhondt S, Shi H, De Milde L, Vanden Bossche R, De Clercq R, Eeckhout D *et al.* 2017. The transcriptional repressor complex FRS7–FRS12 regulates flowering time and growth in Arabidopsis. *Nature Communications* **8**: 15235.

Saedler H, Becker A, Winter KU, Kirchner C, Theissen G. 2001. MADS-box genes are involved in floral development and evolution. *Acta Biochimica Polonica* **48**: 351–358.

Sawa S, Ito T, Shimura Y, Okada K. 1999. *FILAMENTOUS FLOWER* controls the formation and development of Arabidopsis inflorescences and floral meristems. *Plant Cell* **11**: 69–86.

Siegfried KR, Eshed Y, Baum SF, Otsuga D, Drews GN, Bowman JL. 1999. Members of the YABBY gene family specify abaxial cell fate in Arabidopsis. *Development* **126**: 4117–4128.

Sommer H, Beltrán JP, Huijser P, Pape H, Lönnig WE, Saedler H, Schwarz-Sommer Z. 1990. Deficiens, a homeotic gene involved in the control of flower morphogenesis in *Antirrhinum majus*: the protein shows homology to transcription factors. *EMBO Journal* **9**: 605–613.

Song X, Cao X. 2017. Transposon-mediated epigenetic regulation contributes to phenotypic diversity and environmental adaptation in rice. *Current Opinion in Plant Biology* **36**: 111–118.

Stirnberg P, Zhao S, Williamson L, Ward S, Leyser O. 2012. *FHY3* promotes shoot branching and stress tolerance in Arabidopsis in an *AXR1*-dependent manner. *The Plant Journal* **71**: 907–920.

Tanaka W, Toriba T, Hirano H. 2017. Three *TOB 1*-related *YABBY* genes are required to maintain proper function of the spikelet and branch meristems in rice. *New Phytologist* **215**: 825–839.

Tanaka W, Toriba T, Ohmori Y, Yoshida A, Kawai A, Mayama-Tsuchida T, Ichikawa H, Mitsuda N, Ohme-Takagi M, Hirano H-Y. 2012. The *YABBY* gene *TONGARI-BOUSHI1* is involved in lateral organ development and

maintenance of meristem organization in the rice spikelet. *Plant Cell* **24**: 80–95.

Tang W, Ji Q, Huang Y, Jiang Z, Bao M, Wang H, Lin R. 2013. FAR-RED ELONGATED HYPOCOTYL3 and FAR-RED IMPAIRED RESPONSE1 Transcription factors integrate light and abscisic acid signaling in Arabidopsis. *Plant Physiology* **163**: 857–866.

Toriba T, Harada K, Takamura A, Nakamura H, Ichikawa H, Suzaki T, Hirano H-Y. 2007. Molecular characterization the *YABBY* gene family in *Oryza sativa* and expression analysis of *OsYABBY1*. *Molecular Genetics and Genomics* **277**: 457–468.

Wang Y, Wang Y-F, Zhang D-B. 2006. Identification of the rice (*Oryza sativa* L.) mutant msp1-4 and expression analysis of its UDT1 and GAMYB genes. *Zhi Wu Sheng Li Yu Fen Zi Sheng Wu Xue Xue Bao = Journal of Plant Physiology and Molecular Biology* **32**: 527–534.

Wigge PA. 2013. Ambient temperature signalling in plants. *Current Opinion in Plant Biology* **16**: 661–666.

Wu C, Cui K, Wang W, Li Q, Fahad S, Hu Q, Huang J, Nie L, Peng S. 2016. Heat-induced phytohormone changes are associated with disrupted early reproductive development and reduced yield in rice. *Scientific Reports* **6**: 34978.

Wu C, Tang S, Li G, Wang S, Fahad S, Ding Y. 2019. Roles of phytohormone changes in the grain yield of rice plants exposed to heat: a review. *PeerJ* **7**: e7792.

Xie K, Minkenberg B, Yang Y. 2015. Boosting CRISPR/Cas9 multiplex editing capability with the endogenous tRNA-processing system. *Proceedings of the National Academy of Sciences, USA* **112**: 3570–3575.

Xie S, Luo H, Huang Y, Wang Y, Ru W, Shi Y, Huang W, Wang H, Dong Z, Jin W. 2020. A missense mutation in a large subunit of ribonucleotide reductase confers temperature-gated tassel formation. *Plant Physiology* **184**: 1979–1997.

Yamaguchi T, Nagasawa N, Kawasaki S, Matsuoka M, Nagato Y, Hirano H-Y. 2004. The *YABBY* gene *DROOPING LEAF* regulates carpel specification and midrib development in *Oryza sativa*. *Plant Cell* **16**: 500–509.

Yanofsky MF, Ma H, Bowman JL, Drews GN, Feldmann KA, Meyerowitz EM. 1990. The protein encoded by the *Arabidopsis* homeotic gene *agamous* resembles transcription factors. *Nature* **346**: 35–39.

Young Chae G, Hong W-J, Jeong Jang M, Jung K-H, Kim S. 2021. Recurrent mutations promote widespread structural and functional divergence of MULE-derived genes in plants. *Nucleic Acids Research* **49**: 11765–11777.

Yu X, Li L, Li L, Guo M, Chory J, Yin Y. 2008. Modulation of brassinosteroid-regulated gene expression by Jumonji domain-containing proteins ELF6 and REF6 in Arabidopsis. *Proceedings of the National Academy of Sciences, USA* **105**: 7618–7623.

Yuan Z, Persson S, Zhang D. 2020. Molecular and genetic pathways for optimizing spikelet development and grain yield. *aBIOTECH* **1**: 276–292.

Yun D, Liang W, Dreni L, Yin C, Zhou Z, Kater MM, Zhang D. 2013. OsMADS16 genetically interacts with OsMADS3 and OsMADS58 in specifying floral patterning in rice. *Molecular Plant* **6**: 743–756.

Zhang D, Yuan Z. 2014. Molecular control of grass inflorescence development. *Annual Review of Plant Biology* **65**: 553–578.

Zhang T, Li C, Li D, Liu Y, Yang X. 2020. Roles of YABBY transcription factors in the modulation of morphogenesis, development, and phytohormone and stress responses in plants. *Journal of Plant Research* **133**: 751–763.

Zhang Y, Su J, Duan S, Ao Y, Dai J, Liu J, Wang P, Li Y, Liu B, Feng D *et al.* 2011. A highly efficient rice green tissue protoplast system for transient gene expression and studying light/chloroplast-related processes. *Plant Methods* **7**: 30.

Zhu W, Yang L, Wu D, Meng Q, Deng X, Huang G, Zhang J, Chen X, Ferrándiz C, Liang W *et al.* 2022. Rice *SEPALLATA* genes *OsMADS5* and *OsMADS34* cooperate to limit inflorescence branching by repressing the *TERMINAL FLOWER1* -like gene *RCN4*. *New Phytologist* **233**: 1682–1700.

Supporting Information

Additional Supporting Information may be found online in the Supporting Information section at the end of the article.

Fig. S1 Characterization of the rice *tap-1* mutant grown at 30°C.

Fig. S2 Complementation of rice *tap-1* mutant by *proTAP::TAP-GFP*.

Fig. S3 Generation of rice *osyab4* and *osyab5* mutants using CRISPR/Cas9 technology.

Fig. S4 *TAP*, *OsYAB4*, and *OsYAB5* function together to regulate rice panicle and spikelet development under 28°C.

Fig. S5 *TAP*, *OsYAB4*, and *OsYAB5* function together to regulate rice panicle and spikelet development under 34°C.

Table S1 Primers and target sequence used in this study.

Table S2 Settings of different growth chambers used in the characterization of the rice mutant phenotypes.

Table S3 Rice inflorescence characteristics of each allele of *tap* in different environments.

Table S4 Rice spikelet characteristics of each allele of *tap* in different environments.

Table S5 GO terms enriched using overlapping DEGs between two different stages of rice panicle development at HT condition.

Table S6 GO terms enriched using overlapping DEGs between two different stages of rice panicle development at LT condition.

Table S7 List of meristem development, flower development, and cell differentiation-related genes in downregulated DEGs in rice *tap-1* mutant.

Please note: Wiley is not responsible for the content or functionality of any Supporting Information supplied by the authors. Any queries (other than missing material) should be directed to the *New Phytologist* Central Office.